

Bayesian functional data analysis in astronomy

Thomas Loredo ¹ *, Tamás Budavári ² , David Kent ³ , and David Ruppert ⁴ 

¹ Cornell Center for Astrophysics and Planetary Science and Department of Statistics and Data Science, Cornell University; loredo@astro.cornell.edu

² Department of Applied Mathematics and Statistics, Johns Hopkins University; budavari@jhu.edu

³ Department of Statistics and Data Science, Cornell University; dk657@cornell.edu

⁴ School of Operations Research and Information Engineering and Department of Statistics and Data Science, Cornell University; dr24@cornell.edu

* Correspondence: loredo@astro.cornell.edu

Abstract: Cosmic demographics—the statistical study of populations of astrophysical objects—has long relied on *multivariate statistics*, providing methods for analyzing data comprising fixed-length vectors of properties of objects, as might be compiled in a tabular astronomical catalog (say, with sky coordinates, and brightness measurements in a fixed number of spectral passbands). But beginning with the emergence of automated digital sky surveys, ca. 2000, astronomers began producing large collections of data with more complex structure: light curves (brightness time series) and spectra (brightness vs. wavelength). These comprise what statisticians call *functional data*—measurements of populations of functions. Upcoming automated sky surveys will soon provide astronomers with a flood of functional data. New methods are needed to accurately and optimally analyze large ensembles of light curves and spectra, accumulating information both along and across measured functions. Functional data analysis (FDA) provides tools for statistical modeling of functional data. Astronomical data presents several challenges for FDA methodology, e.g., sparse, irregular, and asynchronous sampling, and heteroscedastic measurement error. Bayesian FDA uses hierarchical Bayesian models for function populations, and is well suited to addressing these challenges. We provide an overview of astronomical functional data, and of some key Bayesian FDA modeling approaches, including functional mixed effects models, and stochastic process models. We briefly describe a Bayesian FDA framework combining FDA and machine learning methods to build low-dimensional parametric models for galaxy spectra.

Keywords: astrostatistics; time series; spectroscopy; Bayesian data analysis; functional data analysis; hierarchical Bayesian modeling; Gaussian processes; dimension reduction; manifold learning

1. Introduction

For centuries, astronomers contemplating the properties of stellar populations relied on data collected in *tabular stellar catalogues*. Ptolemy's second century *Almagest* contains some of the earliest such tables, with columns containing instructions for finding a star in a specified constellation, the star's ecliptic longitude and latitude, and the star's brightness as an integer magnitude, from 1 to 6, bright to dim (popularizing a perceptual system that evolved to become the modern and somewhat peculiar magnitude system). By the early twentieth century, astronomers produced many more extensive and diverse tabular catalogs, describing basic properties of stars, galaxies, nebulae, minor planets, and other families of objects.

At the turn of the twenty-first century, the first large-scale automated digital sky survey, the *Sloan Digital Sky Survey* (SDSS), began producing vast tabular catalogs, dwarfing the scale of previous catalogs. For example, the SDSS PhotoObjA11 table reports measurements of nearly a half-billion stars and galaxies imaged in the northern sky, in a table with over 500 columns, accessible to astronomers via an SQL-like database. Among the columns are coordinate and magnitude measurements (“photometry”) akin to those of the *Almagest*,

Citation: Loredo, T.; Budavári, T.; Kent, D.; Ruppert, D. Bayesian functional data analysis in astronomy. *Phys. Sci. Forum* **2024**, *1*, 0. <https://doi.org/>

Published:

Copyright: © 2024 by the authors. Submitted to *Phys. Sci. Forum* for possible open access publication under the terms and conditions of the Creative Commons Attribution (CC BY) license (<https://creativecommons.org/licenses/by/4.0/>).

albeit far more precisely defined and measured (and, importantly, supplemented with uncertainties). Magnitude measurements are available in various spectroscopic bandpasses, providing quantification of the colors of objects. The measurements also include low-dimensional parametric descriptions of the shapes of galaxies, derived from the underlying spatially-resolved image data.

The early twentieth century catalogs motivated the development of what was initially called “statistical astronomy”—the study of *populations* of astronomical objects, as groups, via the techniques of multivariate statistics and spatial statistics, i.e., techniques for modeling *vector-valued data*. Today, “statistical astronomy” is used more broadly, referring to any use of formal statistical methods in astronomy. We use *cosmic demographics* specifically for statistical study of astronomical populations, typically based on survey data summarized in catalogs. Classic examples of cosmic demography tasks and tools include:

- Density estimation, e.g., estimating the distribution of apparent or intrinsic brightness of a stellar or galaxy population;
- Spatial statistics, e.g., the invention of the Neyman-Scott process to model the spatial clustering of galaxies [1];
- Multivariate regression, e.g., for calibrating stellar and galaxy luminosity indicators (functions of observables that predict luminosity);
- Discovery of structure in multivariate distributions such as clusters or sequences (reduced-dimension manifolds), via tools such as principal component analysis (PCA) or *k*-nearest neighbors.

Importantly, besides its tabular photometric catalogs, SDSS produced other large collections of non-tabular data: spectroscopic and image databases. These databases report observations of *functions*: one-dimensional spectra (observed light flux vs. wavelength) in spectroscopic databases, and two-dimensional images (flux vs. sky coordinates) in image databases. Of course, such measurements long predate SDSS; e.g., quantitative spectroscopy transformed astronomy to astrophysics beginning in the late nineteenth century. But SDSS made large samples of calibrated spectra and images available to the astronomical community for the first time, enabling demographic modeling of spectrum and image ensembles at an unprecedented scale.

Where classical cosmic demographics viewed the sky as full of *vectors*, modern cosmic demographics is beginning to view the sky as full of *functions*.

A similar change in the character of data ensembles occurred about a decade earlier in other fields, leading to the creation of a relatively new area of statistics, *functional data analysis* (FDA): statistical analysis of measurements of ensembles of related functions. Astronomers have only recently begun adapting techniques from the FDA literature to astronomy. In this perspective contribution to the MaxEnt 2024 proceedings issue of *Physical Sciences Forum*, we provide a brief overview of FDA (§ 2), highlight recent FDA applications in astronomy (§ 3), and describe an illustrative example from our research on Bayesian FDA: developing a low-dimensional parametric model for the population of galaxy spectra observed by SDSS (§ 4).

2. Functional data analysis

FDA seeks to discover and exploit patterns in the shapes of functions across an ensemble in a manner that accounts for diversity across the ensemble. Important motivating examples in astronomy include:

- Characterizing the diversity of light curves for variable and transient sources, e.g., for calibrating or generalizing the Leavitt period-luminosity law for Cepheids, or the luminosity-time scale law for Type Ia supernova, accounting for patterns and diversity in light curve shapes.
- Characterizing the diversity of galaxy spectra, e.g., to enable estimation of galaxy redshifts—Doppler shifts from cosmological expansion that provide distance estimates—from multiband magnitude measurements that provide significant but crude constraints on galaxy spectra (photometric redshifts).

To set the stage for a discussion of FDA for astronomy, here we review key aspects of the nature of functional data, and themes appearing in FDA modeling of such data.

2.1. Functional data

Functional data comprise *measurements of many related functions*, related in the sense of being associated with sources considered to comprise a statistical population or ensemble. In contrast to the vector data that is the subject of multivariate statistics, functional data *may not be of fixed size* across the measured population. Further, the data from each member function typically have a *topology* (a sense of proximity), reflecting that the argument of the measured functions is continuous (e.g., time, wavelength, or spatial coordinates). In contrast, the components of vector data often have no natural notion of order or proximity (e.g., between magnitude and direction data in a tabular catalog).

Most of the FDA literature in statistics focuses on univariate functions. In astronomy, univariate functional data could comprise light curves (functions of time, $f(t)$), or spectra (functions of wavelength, $f(\lambda)$). Functional data can pertain to multivariate functions; such cases are sometimes labeled “next generation” FDA problems. In astronomy, two-dimensional functional data arises in observations of dynamic (time-dependent) spectra, $f(\lambda, t)$, or of images of a class of extended objects, with $f(x, y)$ denoting image intensity as a function of spatial or angular coordinates.

In most cases, functional data are modeled as measurements of an unknown function at a set of specified sample points, e.g., light curves measured at a set of epochs, or spectra measured at a set of wavelengths corresponding to spectroscopic pixels. But in some cases functional data comprise measurements of *functionals* of an underlying function, in the sense of functional analysis (with linear functionals represented as inner product or convolution integrals). A prevalent example in astronomy is photometric data obtained using multiple spectral bandpasses (filters); the flux expected in one band is the integral of the product of the source spectrum and the system response function for that band. The double meaning of “functional” in such contexts is unfortunate but unavoidable.

Functional data arise in diverse sampling regimes:

- *Sampling density:* The functions may be densely or sparsely sampled. Early FDA literature treated densely sampled data, a prototypical example being a collection of handwritten digits or letters, where the data are so densely sampled that they could almost be considered to be curves rather than discrete sets of measurements. In astronomy, spectra are often densely sampled, but light curves (time series) are often sparsely sampled. Dynamic spectra may be densely sampled in wavelength but sparsely sampled in time.
- *Sample locations:* Across the ensemble, the measurements may be on uniformly-spaced, aligned grids, or they may be at irregular, unaligned, asynchronous sample locations, with different numbers of measurements for each member (typical in astronomy).
- *Sample completeness:* The sampling may be complete across the ensemble (when there are shared grids), or there could be gaps or missing data, with missingness varying across the members. The latter case is common in astronomy.

Functional data are obtained in different measurement error regimes:

- Some functional data may be considered to be effectively noiseless; this was the case for the early prototypical FDA problems mentioned above. In such settings, the statistical aspects of the problem arise solely from statistical description of the ensemble of functions.
- Functional data often has measurement error. Most commonly in the FDA literature, noise is modeled as additive, Gaussian, and homoskedastic (with the same standard deviation for all measurements), though possibly with unknown standard deviation. In astronomy, measurement error is almost always heteroskedastic, though often with known standard deviations. Measurement errors are often Gaussian to a good approximation, but sometimes are more complex (e.g., reflecting Poisson counting uncertainties from photon counting data).

2.2. Functional data analysis

Functional data *analysis* refers to statistical methods tailored for explanatory and predictive modeling using functional data. Typically there is significant diversity in the function shape across the population, requiring use of high-dimensional models.

The fundamental objects being modeled in FDA are continuous functions rather than the fixed- and finite-length vectors of variables that are the subject of multivariate data analysis and spatial statistics. But FDA builds on the methods and intuition of vector-based statistical modeling, exploiting ideas such as basis expansions and Hilbert spaces to link continuous function modeling to working in a vector space.

Key statistical modeling tools used in FDA include:

- Parametric and semiparametric expansions in a *pre-specified basis*, e.g., splines, a Fourier basis (orthogonal sines and cosines), or wavelets.
- *Stochastic process models*, such as Gaussian processes, viewed as population distributions for functions, with the measured functions treated as independent sample paths from the process.
- Expansions in a data-derived basis, typically found using *functional principal components analysis* (FPCA). Conventional PCA arises in multivariate statistics for finding basis vectors for vector-valued data, treated as independently and identically distributed (IID) samples from a multivariate joint density. FPCA arises in FDA for deriving basis functions for a population of functions, treated as sample paths from a stochastic process.
- Dimension reduction and manifold learning, to discover low-dimensional descriptions of a function ensemble, using FPCA or techniques from machine learning.

In some cases (rare in astronomy), functional data measurements are available on a shared dense, aligned grid. In such settings, in principle the function values on the grid may be used for modeling. But the FDA perspective always views the underlying measured object as a continuous function. For example, splines express a function in terms of function values on a grid (the spline nodes). In FDA, the focus is on the continuous representation (e.g., the connected set of cubic polynomials for cubic splines), not on the discrete set of function values that happen to be convenient for expressing that function. In particular, theory pertaining to the accuracy (bias) and variability (variance) of estimates uses the continuous representation for comparing estimates to true functions.

A very common parametric or semiparametric FDA model architecture is a *mixed effects model*, where each function in the population is modeled as the sum of two components:

- A *fixed effect*: A shared, template-like component whose shape is set by a parameter shared across the population (possibly also depending on known covariates/predictors, such as a measured period for time series data).
- A *random effect*: A peculiar, object-specific component specified by parameters values unique to the object, accounting for variability across the population.

The fixed/random terminology originates from frequentist statistics, where only the parameters in the peculiar component are considered “random variables” (in the frequentist sense of varying statistically in repeated sampling). In Bayesian settings, where “random variable” is interpreted more generally to mean “uncertain quantity,” the parameters of both components are random, and the *shared vs. peculiar* terminology seems more apt.

As an example, for function $f_i(x)$ ($i = 1$ to N) observed at locations x_{ij} ($j = 1$ to M_i), a mixed effects model for the measurements d_{ij} may be:

$$d_{ij} = F_i(x_{ij}) + \epsilon_{ij} \quad (1)$$

$$= G(x_{ij}; \beta) + g(x_{ij}; \chi_i) + \epsilon_{ij} \quad (2)$$

with measurement errors ϵ_{ij} , shared parameter β , and peculiar parameters χ_i . Here $G(x_{ij}; \beta)$ is the fixed effect, representing shared template-like behavior across the population, and $g(x_{ij}; \chi_i)$ is the random effect, representing object-specific function behavior. These

functions are typically represented as basis expansions (the parameter vectors are the expansion coefficients). If object-specific covariates are measured—say, a period in a time series context, as arises in analyses of periodic variable star light curves—those covariates may be included in the fixed effect component, so that objects with the same covariate value (rather than all objects) share a common template behavior.

Common inference and prediction tasks in multivariate statistics include estimating the joint distribution of components of the data vector, finding relationships between the components (correlations, regression laws/scaling laws, and conditional distributions), and clustering and classification. FDA replaces estimating the joint distribution of the data vector with learning the distribution for the function population (e.g., as a stochastic process or via some other architecture; see below). For inference of relationships, FDA technology has been developed for a variety of regression tasks involving measured functions and scalar or vector covariates. Scalar- or vector-on-function regression aims to predict a parameter of interest from a measured function; predicting a variable star’s luminosity from its light curve is an astronomical example. Function-on-scalar or -vector regression uses the function as the response rather than predictor, and function-on-function regression uses one type of function to predict another (e.g., using a spectrum to predict a time series).

Bayesian FDA frames FDA tasks within the Bayesian paradigm, where modeling of populations relies on hierarchical Bayesian (HB) methods. Bayesian methods treat unknown parameters as well as data as “random” (in the sense of uncertain a priori), requiring introduction of prior distributions for parameters. In HB population modeling, parameters that describe the population as a whole are dubbed *hyperparameters*, and the prior distribution for such a parameter is sometimes called a hyperprior. Object-specific parameters, not directly observable, are often called *latent parameters*. Whereas a hyperparameter appears only once in an HB model (globally controlling population properties), latent parameters are replicated across the population, so the prior distribution for the latent parameters is a population distribution, i.e., a statistical description of variability across the population. The population distribution typically has parameters of its own; these hyperparameters may in fact be of key interest, describing the diversity of functions across the population.

In the mixed effects model of equation (2), β is a hyperparameter controlling the shared template function, and the N values of χ_i are latent parameters, viewed as drawn from a population distribution that itself may have parameters θ (e.g., a population mean and standard deviation for the χ_i distribution).

Bayesian FDA may instead adopt a *stochastic process* modeling architecture, for example, specifying that the modeled functions may be described as draws from a Gaussian process (GP) [2]. *GP regression*—fitting measurements of a *single* function with a GP—has become popular in astronomy, particularly in time series settings [3]. In a regression setting, where one has data from only a single sample path drawn from the GP, the covariance function controlling the flexibility of the GP must be highly constrained a priori. Typically very simple covariance functions, with just two or three adjustable parameters, are used. In contrast, in GP FDA, data from *many* draws from the GP are analyzed *jointly*. This enables adopting much more flexible GP covariance structures, including nonstationary covariance functions with many parameters.

With either architecture, an important advantage of Bayesian FDA is how the statistical phenomena of shrinkage and borrowing strength arise naturally within a hierarchical Bayesian setup. The joint, fully probabilistic analysis enables accumulation of information both along the paths of individual functions, and across the many paths comprising the function population [4,5]. The sharing of information across paths improves the accuracy with which each individual function can be recovered. And the fully probabilistic framework allow inference at the population level (of hyperparameters, such as parameters defining scaling laws) to account for uncertainties in the individual function estimates more thoroughly than is possible if one were to naively fit or smooth each object’s function data independently, and then use the independent best-fit estimates to characterize the popula-

tion. In fact, in many settings the latter approach is known to be statistically inconsistent, converging away from the truth as the number of objects measured increases.

This overview merely scratches the surface of FDA. Good entry points to the field include the influential early monographs of Ramsay and Silverman and their collaborators [6,7], an FDA handbook [8], and recent review articles [5,9]. For specifically Bayesian FDA methodology, few tutorial works are available; see the review of Morris [5] and the monograph on GP FDA by Shi et al. [2]. Besides covering formal statistical modeling, these works also cover practical FDA tasks such as function registration.

3. FDA in astronomy

As noted in the Introduction, much emerging astronomical data would be recognized as functional data by statisticians, especially large spectroscopic and time series catalogs being produced by current and forthcoming surveys. To date, only rarely have astronomers explicitly drawn on methods in the FDA literature to analyze such data. Of course, in the statistics literature, FDA methodology was not suddenly invented; it arose in response to changes in data modalities, becoming identified as a new subdiscipline worthy of a new name several years after the foundational ideas began appearing. Similarly, astronomers have developed what is essentially FDA technology in response to challenges posed by new functional datasets. For example, Tanvir, Hendry, Kanbur and collaborators developed a technique for fitting the light curves of Cepheid periodic variable stars that is very similar to FPCA [10,11]. Mandel and collaborators developed and continue to refine a model for the population of Type Ia supernova transient light curves that implements Bayesian GP FDA for dynamic spectra (bivariate functions of time and wavelength) [12]. Their work is the most sophisticated FDA application we know of in astronomy, rivaling in complexity the best Bayesian FDA work in the statistics literature.

The earliest explicit use of FDA in astronomy that we are aware of is a study of the light curves of long-period Mira variable stars, reported in the statistics literature by a collaboration led by statistician Woncheol Jang and astronomer Martin Hendry [13]. They used FPCA and functional clustering to identify Mira variables that have periods that change significantly in time. In a more recent collaboration between astronomers and statisticians, Patil et al. used FPCA to analyze nearly 19,000 stellar spectra from SDSS observations of an open star cluster, to quantify the complexity of spectral diversity [14]. Ten functional principal components are needed to characterize the statistically significant diversity, and the FPCA scores can be used to estimate physical parameters describing the chemical composition of stars in the cluster.

Our team is developing FDA methods for four problems:

- Modeling the periodic light curves of Cepheid variable stars using a Fourier mixed-effects model;
- Classification of variable star and transient object light curves via GP-based FDA;
- Modeling temporal variability of stellar spectra due to stellar activity (starspots, plage regions, faculae) by combining FDA and bivariate function approximation using empirical separable expansions;
- Constructing a low-dimensional empirical model for galaxy spectra by modeling SDSS galaxy spectra with a combination of FDA and manifold learning methods.

In the next section we briefly describe the galaxy spectra application.

4. Modeling the population of galaxy spectra

Galaxies have diverse optical spectra (also called spectral energy distributions, or SEDs), reflecting diversity in their stellar populations (which vary in age, mass distribution, and chemical composition), absorption and scattering by dust and gas, and the absence or presence of an active galactic nucleus (AGN), a supermassive central black hole contributing optical emission from an accretion disk and jet formed as surrounding gas is consumed. Physical models for a single galaxy spectrum predict the emission from stellar populations by positing distributions for the masses and compositions of stars at birth, and

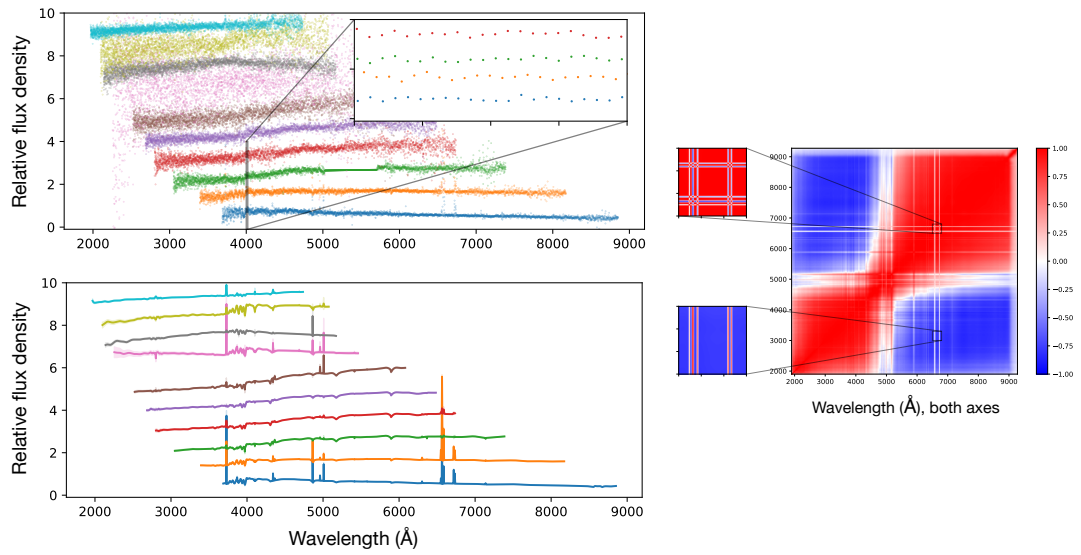


Figure 1. SnL model for the population of SDSS galaxy spectra. *Top:* Measurements of 10 SEDs shown (as dots colored for each SED). *Right:* Covariance function for GP SED population model. *Bottom:* Denoised and interpolated SEDs corresponding to top panel, with error bands (quite narrow for most SEDs; most perceptible for the pink SED).

a distribution of birth times, and then computing the SED as a function of age by accounting for stellar evolution. Such models typically have a dozen or more parameters and they are computationally expensive (recent work is accelerating them via emulation with machine learning algorithms). Fits to low- and modest-resolution spectral data typically exhibit significant parameter degeneracy (nonidentifiability), exacerbated by the possible presence of an AGN component (which can mimic the contribution of some stellar components) [15].

It would be extremely useful to have an accurate and fast low-dimensional model for galaxy SEDs. Such a model probably would not replace physical models for the purpose of estimating physical parameters for particular galaxies. But a fast, low-dimensional model would be very useful for simulating galaxy populations (for the purpose of developing and testing large-scale data analysis pipelines for upcoming surveys). And such a model could be crucial for photometric redshift estimation, where astronomers estimate how much a galaxy's spectrum has been redshifted by cosmological expansion, using only a few bands of photometric data as a crude spectrum measurement for simultaneous estimation of a galaxy's spectrum and the amount of redshift. Redshift serves as a proxy for distance, a crucial galaxy parameter for cosmology. Achieving the science goals of upcoming surveys requires accurate and precise photometric redshift estimation for hundreds of millions of galaxies. Current physical models are too complex and slow for this purpose. Black-box machine learning algorithms are not accurate enough. Photometric redshift estimation using an accurate and fast low-dimensional empirical SED model is a promising approach.

We are building a SED model using nearly 800,000 calibrated high-resolution SEDs observed by SDSS, with known redshifts (from measuring the locations of Doppler-shifted spectral line features). Our framework has three components whose linked operation is depicted in Figures 1 and 2.

The top panel in Fig. 1 shows calibrated SED data for a small selection of SEDs, shifted to the galaxy rest frame using each galaxy's known redshift. The SED data are not aligned, have noise at varying levels, and many spectra have gaps (e.g., the horizontal line in the green SED). We model the collection of SEDs using a B-spline basis for the continuum, and Gaussian functions for the lines, with the basis coefficients and line effective areas drawn from a high-dimensional multivariate normal distribution [16]. This *Splines-n-Lines* (SnL) model corresponds to a nonstationary degenerate Gaussian process (GP) model for the SED population, with a complex mean SED and a nonstationary, richly structured covariance matrix (described with thousands of parameters). The inferred covariance

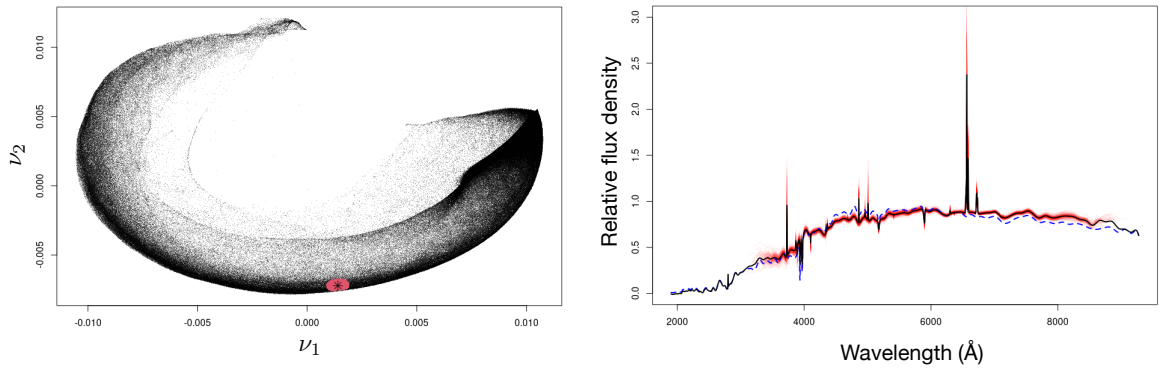


Figure 2. *Left:* PHATE-based manifold for SDSS SEDs; 2D projection of 3D manifold shown, with manifold coordinates (ν_1, ν_2) . *Right:* Example predicted SEDs from inverse map. Black curve shows SED corresponding to manifold coordinates shown by star in left panel. Red curves span show SEDs spanning the red region containing the star in left panel.

function is depicted in the right panel (as a matrix on a finite wavelength grid); it displays how parts of the spectra are related, in particular, how line strengths depend on parts of the continuum. For each SED, SnL estimates a denoised predicted spectrum—the curves in the lower panel—and uncertainties. Notably, it successfully interpolates and extrapolates incomplete SEDs, producing an ensemble of continuous SED estimates with large overlapping wavelength coverage. SnL replaces ad hoc methods for putting SEDs on a common wavelength grid, e.g., via PCA; it provides functional (gridless) representations, explicitly models the connection between lines and the continuum spectrum, and provides uncertainties.

We next use the SnL-produced (gridless) SEDs as inputs for manifold learning algorithms, seeking a low-dimensional representation. Many manifold learning algorithms use a matrix of pairwise similarities to construct a low-dimensional relabeling of the data that approximately preserves distances. We use the SnL-produced SEDs to compute a pairwise SED similarity matrix using cosine similarity. The similarity matrix serves as input to the PHATE manifold learning algorithm [17]. PHATE identifies a 3D manifold in a learned SED manifold coordinate space denoted $\vec{\nu} = (\nu_1, \nu_2, \nu_3)$, shown in a 2D projection in the left panel of Fig. 2. SEDs occupy a thin shell-like structure in the embedding space.

Finally, we build a parametric SED model, using the $\vec{\nu}$ coordinates as SED parameters, by inverting the map from SEDs to the manifold using a new function-on-vector regression algorithm. It uses thin-plate splines as basis functions in $\vec{\nu}$ space to map back to the SnL spline and line coefficients. The right panel shows the SED (black curve) corresponding to the indicated point in $\vec{\nu}$ space, along with several nearby SEDs (red) from the red region of the SED manifold. Moving over the entire space smoothly generates SEDs spanning the full diversity seen by SDSS.

A population distribution in $\vec{\nu}$ space can be used to simulate SEDs without the discreteness imposed by current methods using prototypical SEDs. A photo- z estimation algorithm can be built using the inverse map as a 3-parameter model to fit photometric data via “synthetic photometry”—using a predicted SED to predict the photometry by computing functionals of the spectrum using known photometric response functions.

5. Closing remarks

Current and emerging astronomical instruments place astronomy in the midst of a veritable flood of functional data, across the electromagnetic spectrum. Dedicated exoplanet surveys are producing dynamic spectra at extremely high spectral resolution for thousands of stars; successful detection of Earth-like planets will require careful modeling of stellar activity signals in the data that can mask or mimic planet signals. Orbiting x-ray and gamma-ray instruments are producing time series, spectra, and dynamic spectra for

thousands of sources. The Dark Energy Spectroscopic Instrument (DESI) has begun producing a sample of spectrophotometrically calibrated galaxy spectra that will soon dwarf the SDSS sample. The Rubin Observatory's LSST survey, mentioned in the Introduction, will imminently turn the flood into a torrent; it will produce multiband time series and images of many billions of stars and galaxies, beginning in 2025. These developments surely motivate broader adoption of FDA in astronomy, with Bayesian FDA particularly well suited to handling the complexities of irregular and asynchronous sampling, nontrivial measurement error, and selection effects.

Author Contributions: Conceptualization, T.L., T.B., and D.R.; methodology, D.K., D.R., T.L., and T.B.; software, D.K. and T.L.; writing—original draft preparation, T.L.; writing—review and editing, T.B., D.K., and D.R.; supervision, T.L. and D.R.. All authors have read and agreed to the published version of the manuscript.

Funding: This research was supported by NSF grants AST-1814840, AST-1814840, and DMS-2210790 at Cornell University, and by NSF grants AST-1814778 and AST-2206341 at Johns Hopkins University.

Conflicts of Interest: The authors declare no conflicts of interest.

References

1. Neyman, J.; Scott, E.L. Statistical Approach to Problems of Cosmology. *Journal of the Royal Statistical Society: Series B (Methodological)* **1958**, *20*, 1–29. <https://doi.org/10.1111/j.2517-6161.1958.tb00272.x>.
2. Shi, J.Q.; Choi, T.; Qing Shi, J. *Gaussian Process Regression Analysis for Functional Data*; Chapman & Hall: Boca Raton, 2011.
3. Aigrain, S.; Foreman-Mackey, D. Gaussian Process Regression for Astronomical Time-Series, 2022.
4. Morris, J.S.; Carroll, R.J. Wavelet-based Functional Mixed Models. *Journal of the Royal Statistical Society: Series B (Statistical Methodology)* **2006**, *68*, 179–199. <https://doi.org/10.1111/j.1467-9868.2006.00539.x>.
5. Morris, J.S. Functional Regression. *Annual Review of Statistics and Its Application* **2015**, *2*, 321–359. <https://doi.org/10.1146/annurev-statistics-010814-020413>.
6. Ramsay, J.O.; Silverman, B.W. *Functional Data Analysis*, second ed.; Springer Series in Statistics, Springer, New York, 2005.
7. Ramsay, J.; Hooker, G.; Graves, S. *Functional Data Analysis with R and MATLAB*; Springer New York: New York, NY, 2009. <https://doi.org/10.1007/978-0-387-98185-7>.
8. Ferraty, F.; Romain, Y., Eds. *The Oxford Handbook of Functional Data Analysis*; Oxford University Press: New York, 2011.
9. Wang, J.L.; Chiou, J.M.; Müller, H.G. Functional Data Analysis. *Annual Review of Statistics and Its Application* **2016**, *3*, 257–295. <https://doi.org/10.1146/annurev-statistics-041715-033624>.
10. Tanvir, N.R.; Hendry, M.A.; Watkins, A.; Kanbur, S.M.; Berdnikov, L.N.; Ngeow, C.C. Determination of Cepheid Parameters by Light-Curve Template Fitting. *Monthly Notices of the Royal Astronomical Society* **2005**, *363*, 749–762. <https://doi.org/10.1111/j.1365-2966.2005.09466.x>.
11. Kanbur, S.M.; Iono, D.; Tanvir, N.R.; Hendry, M.A. On the Use of Principal Component Analysis in Analysing Cepheid Light Curves. *Monthly Notices of the Royal Astronomical Society* **2002**, *329*, 126–134. <https://doi.org/10.1046/j.1365-8711.2002.04948.x>.
12. Mandel, K.S.; Thorp, S.; Narayan, G.; Friedman, A.S.; Avelino, A. A Hierarchical Bayesian SED Model for Type Ia Supernovae in the Optical to Near-Infrared. *Monthly Notices of the Royal Astronomical Society* **2022**, *510*, 3939–3966. <https://doi.org/10.1093/mnras/stab3496>.
13. Park, C.; Ahn, J.; Hendry, M.; Jang, W. Analysis of Long Period Variable Stars With Nonparametric Tests for Trend Detection. *Journal of the American Statistical Association* **2011**, *106*, 832–845. <https://doi.org/10.1198/jasa.2011.ap08689>.
14. Patil, A.A.; Bovy, J.; Eadie, G.; Jaimungal, S. Functional Data Analysis for Extracting the Intrinsic Dimensionality of Spectra: Application to Chemical Homogeneity in the Open Cluster M67. *The Astrophysical Journal* **2022**, *926*, 51. <https://doi.org/10.3847/1538-4357/ac35d6>.
15. Pacifici, C.; Iyer, K.G.; Mobasher, B.; da Cunha, E.; Acquaviva, V.; Burgarella, D.; Rivera, G.C.; Carnall, A.C.; Chang, Y.Y.; Chartab, N.; et al. The Art of Measuring Physical Parameters in Galaxies: A Critical Assessment of Spectral Energy Distribution Fitting Techniques, 2022, [arXiv:astro-ph/2212.01915]. <https://doi.org/10.48550/arXiv.2212.01915>.
16. Kent, D.; Budavári, T.; Loredó, T.J.; Ruppert, D. Splines 'n Lines: Rest-frame Galaxy Spectral Energy Distributions via Bayesian Functional Data Analysis, 2023, [2310.19340].
17. Moon, K.R.; van Dijk, D.; Wang, Z.; Gigante, S.; Burkhardt, D.B.; Chen, W.S.; Yim, K.; van den Elzen, A.; Hirn, M.J.; Coifman, R.R.; et al. Visualizing Structure and Transitions in High-Dimensional Biological Data. *Nature Biotechnology* **2019**, *37*, 1482–1492. <https://doi.org/10.1038/s41587-019-0336-3>.

Disclaimer/Publisher's Note: The statements, opinions and data contained in all publications are solely those of the individual author(s) and contributor(s) and not of MDPI and/or the editor(s). MDPI and/or the editor(s) disclaim responsibility for any injury to people or property resulting from any ideas, methods, instructions or products referred to in the content.